Environmental Science & Technology

Article

pubs.acs.org/est

Sunlight Promotes Fast Release of Hazardous Cadmium from Widely-Used Commercial Cadmium Pigment

Huiting Liu,[†] Han Gao,[†] Mingce Long,[‡] Heyun Fu,[†] Pedro J. J. Alvarez,[§] Qilin Li,[§] Shourong Zheng,[†] Xiaolei Qu,[*,†] and Dongqiang Zhu[∥]

[†]State Key Laboratory of Pollution Control and Resource Reuse, School of the Environment, Nanjing University, Jiangsu 210023, China

[‡]School of Environment Science and Engineering, Shanghai Jiao Tong University, Shanghai 200240, China

[§]Department of Civil and Environmental Engineering, Rice University, Houston, Texas 77005, United States

[∥]School of Urban and Environmental Sciences, Peking University, Beijing 100871, China

Supporting Information

ABSTRACT: Cadmium pigments are widely used in the polymer and ceramic industry. Their potential environmental risk is under debate, being the major barrier for appropriate regulation. We show that 83.0 ± 0.2% of hazardous cadmium ion (Cd^{2+}) was released from the commercial cadmium sulfoselenide pigment (i.e., cadmium red) in aqueous suspension within 24 h under simulated sunlit conditions. This photodissolution process also generated sub-20 nm pigment nanoparticles. Cd^{2+} release is attributed to the reactions between photogenerated holes and the pigment lattices. The photodissolution process can be activated by both ultraviolet and visible light in the solar spectrum. Irradiation under alkaline conditions or in the presence of phosphate and carbonate species resulted in reduced charge carrier energy or the formation of insoluble and photostable cadmium precipitates on pigment surfaces, mitigating photodissolution. Tannic acid inhibited the photodissolution process by light screening and scavenging photogenerated holes. The fast release of Cd^{2+} from the pigment was further confirmed in river water under natural sunlight, with 38.6 ± 0.1% of the cadmium released within 4 h. Overall, this study underscores the importance to account for photochemical effects to inform risk assessments and regulations of cadmium pigments which are currently based on their low solubility.

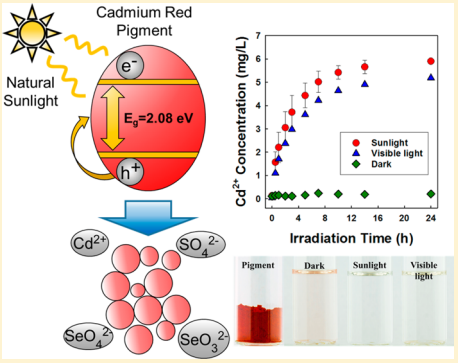

INTRODUCTION

Cadmium pigments, including cadmium sulfide, cadmium selenide, and cadmium sulfoselenide, are widely used in the polymer and ceramic industries owing to their heat stability, chemical resistance, dispersibility, opacity, tinting strength, and brilliance.[1,2] They are especially preferred in processes or applications involving elevated temperatures in which organic pigments are unstable. The annual global consumption of cadmium pigments exceeds 2500 tons, with 90% used in plastics and 9% in ceramics.[2] There is a long debate on whether cadmium pigments pose a genuine risk to human health and the environment.[1,2] Cadmium ion (Cd^{2+}) is known to cause acute toxicity based on short-term animal tests, and is a probable human carcinogen.[3] Thus, the dissolution of cadmium pigments and consequent release of hazardous Cd^{2+} are key processes that control their potential environmental impacts. Previous risk assessments suggested that the use of cadmium pigments poses little risk to humans and the environment (except in occupational settings) due to their extremely low solubility ($K_{sp,CdS} = 7.94 \times 10^{-27}$ and $K_{sp,CdSe} = 6.31 \times 10^{-36}$),[4] and consequently low bioavailability.[5−8] Because of insufficient fate, transport, and toxicological studies, current cadmium pigment regulations are based on the precautionary principle.[1] For example, the European Union (EU) prohibits the use of cadmium pigments in 16 plastics with exemptions (see Regulation No. 494/2011). In China and EU, cadmium pigments are recommended to pass extraction tests for Cd^{2+}, < 0.1 wt % (Standards ISO 4620:1986, BS 6857−1987, and HG 2351−1992). However, these presumably conservative regulations may still underestimate associated risks by overlooking photochemical processes that enhance Cd^{2+} release.

The band gap of CdS and CdSe are 2.5 and 1.8 eV, respectively.[9] Cadmium sulfoselenide is the solid solution of CdS and CdSe, whose color can be fine-tuned from orange to red by increasing the amount of selenium.[2,10] Its band gap decreases from 2.5 to 1.8 eV with increasing Se content.[9,11] Thus, cadmium pigments are photoactive under sunlight and are proposed to be used in photovoltaic devices to harvest solar energy.[12,13] However, for many metal-containing semiconduc-

Received: February 4, 2017
Revised: May 13, 2017
Accepted: May 16, 2017
Published: May 16, 2017

DOI: 10.1021/acs.est.7b00654
Environ. Sci. Technol. 2017, 51, 6877−6886

tor photocatalysts, a photocorrosion process will lead to the dissolution and consequent release of metals.[14−19]

Photocorrosion of CdS and CdSe nanoparticles/quantum dots and subsequent release of Cd^{2+} were investigated in previous studies.[14,15,20−27] The process can be induced by oxidative phototransients including photogenerated holes and reactive oxygen species (ROS). However, these studies were carried out using cadmium chalcogenide nanoparticles mostly in simple solution chemistry, and cannot be extrapolated to infer on the behavior of commercial cadmium pigments in natural settings. The photodegradation of CdS pigment in air has also been studied by analyzing historical oil paintings in aim to minimize their deterioration process.[28−30] The discoloration of CdS pigment was attributed to photoinduced oxidation over centuries, which yielded $CdSO_4{\cdot}xH_2O$ and other cadmium species (e.g., $CdCO_3$) by secondary reactions. Nevertheless, our understanding of the photodissolution process of modern commercial cadmium pigments in natural aquatic systems is still limited, which hinders risk assessment and science-based regulation of these pigments and related colored consumer products.

Herein, we examine the photodissolution of a commercial cadmium sulfoselenide pigment (i.e., cadmium red) under simulated sunlight at neutral pH, mimicking natural conditions. The band gap of the pigment and the phototransients generated during irradiation were determined to understand its photochemistry within the solar spectrum. The influence of solution chemistry including pH, phosphate, carbonate, and tannic acid on the photodissolution kinetics was further examined to inform the environmental release process. The photodissolution of cadmium pigments was also examined in river water under natural sunlit conditions to corroborate our findings. In addition to discerning the photoinduced dissolution mechanism, we underscore the importance to consider photochemical processes to accurately assess the associated risks and inform the regulatory process.

MATERIALS AND METHODS

Commercial cadmium sulfoselenide pigment powder (cadmium red) was purchased from Kela Co., Ltd., China. Dimethyl sulfoxide (DMSO, ≥ 99.0%), sodium chloride (NaCl, ≥ 99.5%), sodium carbonate (Na_2CO_3, ≥ 99.8%), sodium thiosulfate pentahydrate ($Na_2S_2O_3{\cdot}5H_2O$, ≥ 99%) and sodium sulfate (Na_2SO_4, ≥ 99%) were purchased from Nanjing Chemical Reagent Co., Ltd., China. 5,5-Dimethyl-1-pyrroline-*N*-oxide (DMPO, ≥ 97%) was obtained from J&K Scientific Ltd., U.S.A. Sodium selenite (Na_2SeO_4, ≥ 98%) was purchased from Chengdu Micxy Chemical Co., Ltd., China. Methyl viologen dichloride hydrate (MV^{2+}, ≥ 98%), sodium phosphate (Na_3PO_4, 96%), sodium selenite pentahydrate ($Na_2SeO_3{\cdot}5H_2O$, ≥ 90%), 2,3-bis(2-methoxy-4-nitro-5-sulfophenyl)-2*H*-tetrazolium-5-carboxanilide (XTT, > 90%), terephthalic acid (TPA, 98%), *N*,*N*-diethyl-*p*-phenylenediamine sulfate salt (DPD, ≥ 99%), and horseradish peroxidase (HRP, ≥ 250 units/mg) were purchased from Sigma-Aldrich, U.S.A. Tannic acid (95%) was purchased from Acros Organics, U.S.A. All solutions were prepared using deionized water (18.2 MΩ·cm at 25 °C) obtained from an ELGA Labwater system (PURELAB Ultra, ELGA LabWater Global Operations, U.K.).

Irradiation Experiments. The stock suspension of commercial cadmium sulfoselenide pigment was prepared by mixing 10 mg pigment with 100 mL deionized water and sonicated using a flat-tip probe sonicator (JY92-IIN, Ningbo Scientz Biotechnology Co., Ltd., China) for 10 min. The sonication probe was operated at a power of 65 W with a mode of five-second sonication and five-second pause.

The sunlight irradiation was simulated by a 50 W Xe lamp (CEL-HXF300, AULTT, China) shining from the top of a cylindrical cell which was equipped with a water-circulating jacket at 20 ± 0.1 °C (DC0506, Shanghai FangRui Instrument Co., Ltd., China). The irradiation energy at the water surface was 202 mW/cm^2 as measured by a radiometer (CEL-NP2000-2, AULTT). The detailed information regarding the irradiation system can be found in Figure S1 of the Supporting Information. The lamp spectrum was similar to that of natural sunlight with the wavelength >300 nm as measured by a spectrometer (USB2000+, Ocean Optics, FL, U.S.A.) (Figure S2). In the irradiation experiments, 20 milliliter cadmium sulfoselenide pigment stock suspension (100 mg/L) and 10 mL NaCl stock solution (20 mM) were mixed and diluted to 200 mL with deionized water in a 250 mL beaker, yielding a suspension containing 10 mg/L cadmium sulfoselenide pigment and 1 mM NaCl. The beaker was then placed in the cylindrical cell for temperature control. The suspension was stirred at 100 rpm during the irradiation experiments. NaCl added in the suspension was used to simulate the ionic strength in freshwater systems. The unadjusted pH of the mixture was 6.77 ± 0.33. During the irradiation, 4 mL suspension was withdrawn periodically from the beaker and filtered using ultrafiltration membranes (Amicon Ultra-15 3 kDa, Millipore, MA, U.S.A.) to separate the dissolved ions from the particles. The Cd^{2+} concentration was determined by atomic absorption spectrophotometry (AAS, M6, Thermo, U.S.A.). The concentrations of other ions presented in irradiated pigment suspensions were determined by ion chromatography (ICS-1000, Dionex, U.S.A.) with a Dionex IonPac AS11-HC analytical column (250 × 4 mm). Dark controls were carried out in the same experimental setting with the Xe lamp off and the beaker wrapped with aluminum foil. In some irradiation experiments, different reagents (CO_3^{2-}, PO_4^{3-}, and tannic acid) and scavengers ($Na_2S_2O_3$ and MV^{2+}) were added in the reaction suspension.

The photodissolution kinetics was also measured in a natural water sample under solar irradiation. The freshwater sample was collected from a river in Yixing, China (N31°15′37.56″, E119°53′28.61″). The sample was filtered through 0.45-μm membranes (Pall, U.S.A.) and stored at 4 °C before use. Solar irradiation was carried out in the same experimental installation without temperature control on the campus of Nanjing University in Nanjing, Jiangsu, China (N32°07′15.27″, E118°56′49.63″) from 11 a.m. to 3 p.m. on 11/04/2016.

Characterization of Cadmium Sulfoselenide Pigment. The size and morphology of pigment particles were analyzed using a scanning electron microscope (SEM, S-3400N II, Hitachi, Japan) and a transmission electron microscope (TEM, JEM-200CX, JEOL, Japan). The elemental composition of the pigment was determined by an inductively coupled plasma mass spectrometry (ICP-MS, NexIon300X, PerkinElmer, U.S.A.) after microwave digestion (ETHOS UP, Milestone, Italy). The structure of pigment was examined using an X-ray powder diffractometer (XRD, D8 Advance, AXS, Germany) and an X-ray photoelectron spectroscopy (XPS, PHI 5000 VersaProbe, UlVAC-PHI, Japan). The XRD pattern was acquired between 20° to 60° in 2θ mode using with Cu Kα radiation at room temperature. The XPS analyses were performed using the monochromatic Al Kα X-ray source and

DOI: 10.1021/acs.est.7b00654
Environ. Sci. Technol. 2017, 51, 6877−6886

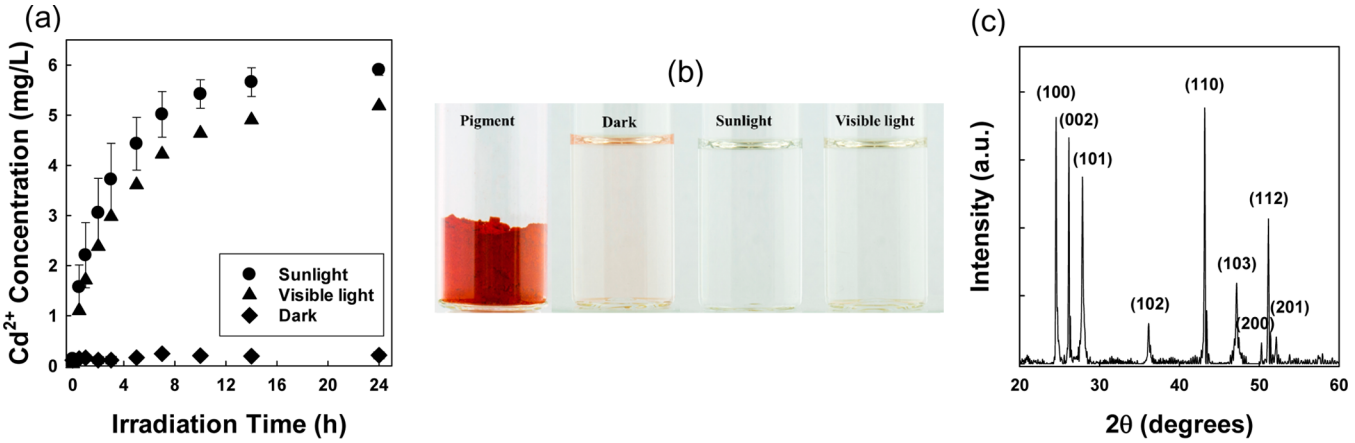

Figure 1. (a) Cadmium release kinetics of 10 mg/L commercial cadmium sulfoselenide pigment in 1 mM NaCl solution at initial pH of 6.77 ± 0.33 under dark, simulated sunlight (202 mW/cm^2), and visible light irradiation (152 mW/cm^2). Error bars represent ± one standard deviation from the average of triplicate tests; (b) photos of the commercial cadmium sulfoselenide pigment sample used in this work and its suspension (10 mg/L) in 1 mM NaCl solution after 24 h under dark, simulated sunlight, and visible light conditions; and (c) XRD spectrum of commercial cadmium sulfoselenide pigment.

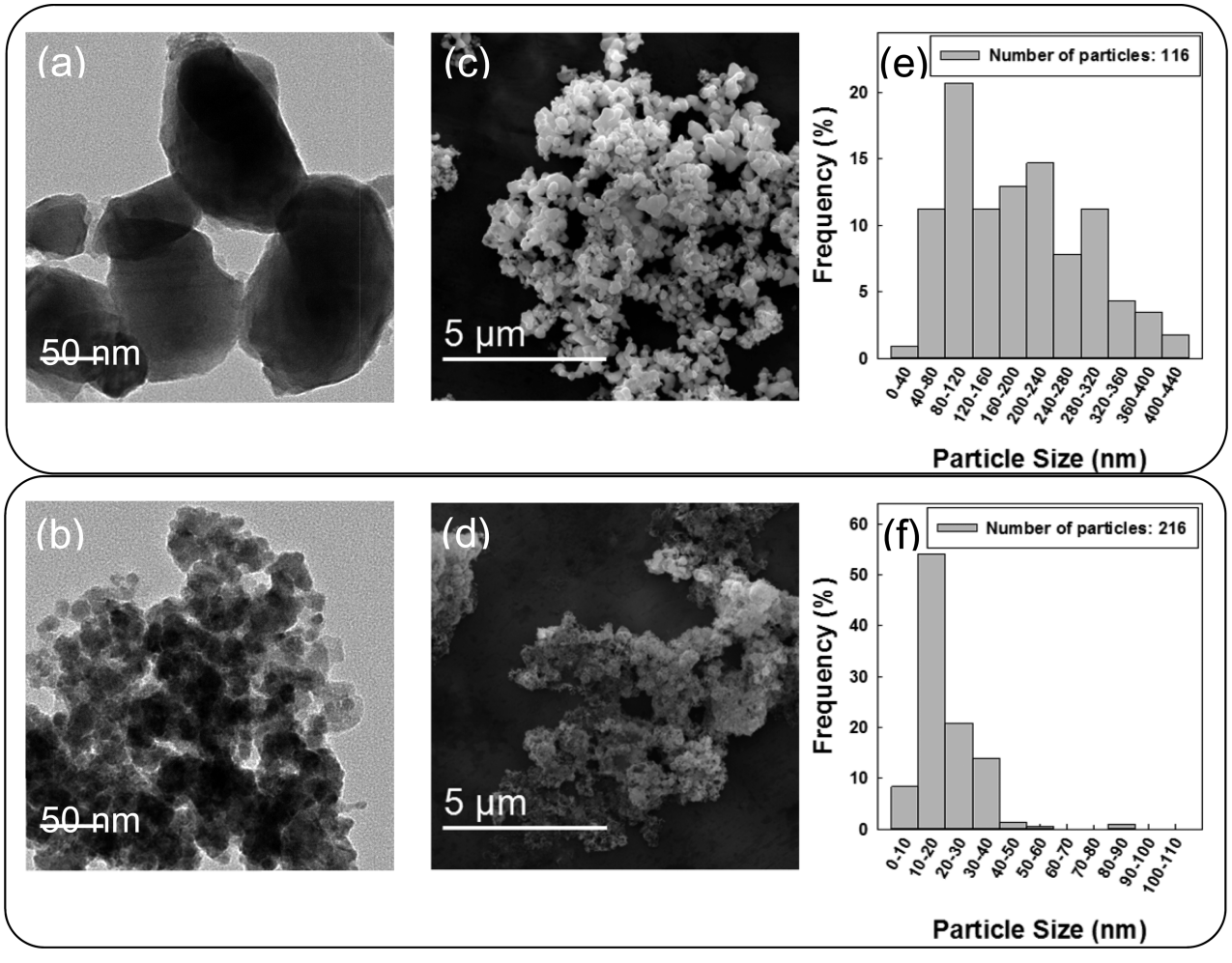

Figure 2. Morphology and size distribution of commercial cadmium sulfoselenide pigment particles before and after 7-h simulated sunlight exposure. TEM micrographs of commercial cadmium sulfoselenide pigment particles (a) before and (b) after sunlight exposure; SEM micrographs of commercial cadmium sulfoselenide pigment particles (c) before and (d) after sunlight exposure; and size distribution of commercial cadmium sulfoselenide pigment particles (e) before and (f) after sunlight exposure based on TEM micrographs.

the spectrometer was calibrated to the position of the $3d_{5/2}$ line of sputtered-clean Ag. The diffuse reflectance ultraviolet−visible spectroscopy (DRS) spectrum of the pigment powder was collected by a SHIMAD UV-3600 UV−vis spectrometer referenced by $BaSO_4$. The Mott−Schottky plot of the pigment was measured using an electrochemical analyzer (CHI 760E,

DOI: 10.1021/acs.est.7b00654
Environ. Sci. Technol. 2017, 51, 6877−6886

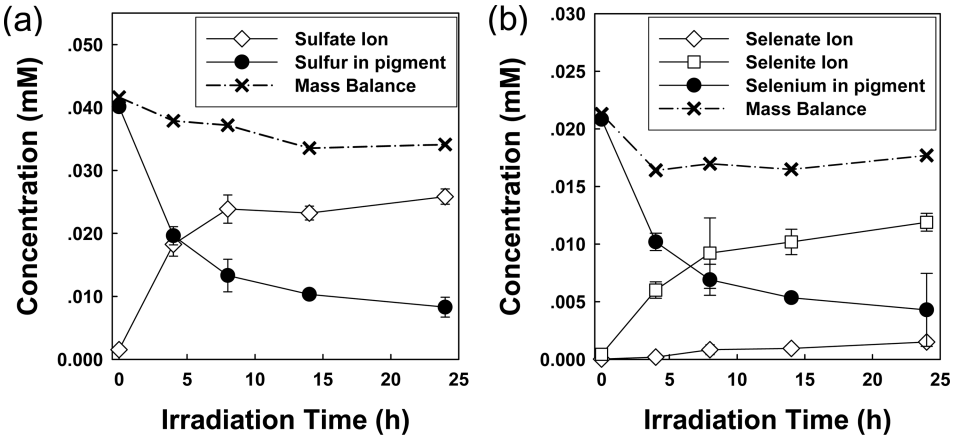

Figure 3. (a) The concentrations and mass balance of sulfur species, including sulfur in the pigment and sulfate ion (SO_4^{2-}), as a function of simulated sunlight irradiation time at initial pH of 6.77 ± 0.33. (b) The concentrations and mass balance of selenium species, including selenium in the pigment, selenite ion (SeO_3^{2-}), and selenate ion (SeO_4^{2-}), as a function of simulated sunlight irradiation time.

CH instrument, China). The impedance−potential tests were taken in a three-electrode setup with a platinum wire as the counter electrode and the saturated calomel electrode (SCE) as the reference electrode. The working electrode was prepared by casting the commercial cadmium sulfoselenide suspension (0.2 g/L in ethanol) over a clean indium tin oxide (ITO) glass plate (Huanan Xiangcheng Co., Ltd., China, 2.5 × 2.5 cm^2, 1.1 mm thick, sheet resistance of 6−8 Ω/in^2). The electrode was then dried at 60 °C for 2 h. The electrolyte was 0.5 M Na_2SO_4 aqueous solution with pH of 5.5. The ac amplitude and frequency were set to be 5 mV and 1.5 kHz, respectively. The ζ-potential of the pigment particles was measured by phase analysis light scattering (PALS) using a ZEN 3500 Zetasizer Nano ZS (Malvern, Worcestershire, U.K.). Each sample was measured five times at 25 °C in a folded capillary cell (Malvern, Worcestershire, U.K.).

ROS Determination. The production of superoxide ($O_2^{\bullet-}$), hydroxyl radical (•OH), and hydrogen peroxide (H_2O_2) by pigment suspensions was measured using probe molecules as described previously.[31−35] Superoxide generation was quantified by the formation of XTT formazan from XTT at an initial concentration of 0.05 mM. XTT formazan was quantified by its absorption at 475 nm using a UV−vis spectra. The extinction coefficient of XTT formazan is 21600 $M^{-1}cm^{-1}$.[31,34] Hydroxyl radical production was quantified by monitoring the degradation of *p*CBA.[32−34] The *p*CBA concentration was measured at a detection wavelength of 254 nm using a high performance liquid chromatography (HPLC, Agilent 1100, Agilent Technologies, U.S.A.) with a Zorbax Eclipse XDB-C18 column (Agilent). The mobile phase was 30% acetonitrile and 70% 0.1 wt % phosphoric acid at a flow rate of 1 mL/min. H_2O_2 generation was measured by the HRP (5 mg/L) catalyzed oxidation of DPD (1 mM).[35] The stable oxidation product, $DPD^{\bullet+}$, was measured by the UV−vis absorbance at 551 nm. The spin-trapping electron spin resonance (ESR) spectra were recorded on a Bruker EMX-10/12 spectrometer (Germany) at room temperature with X-band, microwave power of 20 mW, sweep width of 200 G, modulation width of 1 G, modulation frequency of 100 kHz.

RESULTS AND DISCUSSION

Simulated Sunlight Exposure Results in Rapid Release of Cd^{2+} from Commercial Cadmium Sulfoselenide Pigment.

The dissolution kinetics of a representative cadmium pigment, cadmium sulfoselenide (CdS_xSe_{1-x}) was examined to assess its ability to release hazardous Cd^{2+}. The commercial cadmium sulfoselenide pigment used here was a fine powder with brilliant red color (Figure 1). The SEM and TEM micrographs showed that pigment particles were quasi-spherical with a number-average diameter of 186.1 ± 95.8 nm based on TEM micrographs (Figure 2). The commercial pigment can be readily dispersed in water (Figure 1b). The observed colloidal stability can be attributed to the small size and negative surface charge of the pigment particles with a ζ-potential of −24.37 ± 1.48 mV (electrophoretic mobility of −1.91 ± 0.12 μm·cm/(V s)), which facilitates their colloidal stability through electrostatic repulsion as suggested by the Derjaguin−Landau−Verwey−Overbeek theory.[36,37] The XRD pattern of the commercial pigment is shown in Figure 1c. The XRD spectrum has sharp peaks corresponding to the crystal structure of cadmium sulfoselenide, including 2θ at 24.66° (100), 26.28° (002), 27.99° (101), 36.34° (102), 43.30° (110), 47.28° (103), 50.38° (200), 51.28° (112), and 52.19° (201).[12,38] ICP-MS measurements suggested the atomic ratio of S:Se of the pigment was 1.9 ± 0.1.

The release kinetics of Cd^{2+} from cadmium sulfoselenide pigment was determined under both dark and simulated sunlight irradiation (Figure 1a, see the release kinetics for other cadmium sulfoselenide pigments from different vendors in Figure S3). A small amount of Cd^{2+}, 0.21 ± 0.07 mg/L (<3.0% of the total Cd), was released in the dark condition within 24 h. It can be attributed to the dissolution of cadmium sulfoselenide or the Cd^{2+} release during the dispersion process by sonication. Considering the extremely low solubility of CdS (solubility product constant, K_{sp} = 7.94 × 10^{-27}) and CdSe (K_{sp} = 6.31 × 10^{-36}),[4] the majority of Cd^{2+} released in dark condition is expected to be the latter. However, fast and significant release of Cd^{2+} was observed in the presence of simulated sunlight. The concentration of Cd^{2+} in the suspension increased to 5.01 ± 0.45 mg/L within a 7-h irradiation, and to 5.90 ± 0.10 mg/L at the end of the 24-h irradiation test. This means that 83.0 ± 0.2% of the total cadmium was released, far exceeding the 0.1% limit stipulated by ISO Standard 4620:1986. The pseudo-second-order reaction rate constant was 3.0 L/(mmol·h) (R^2 = 0.93), 334 times higher than that under dark conditions. The rate constant decreased from 3.0 to 1.5 L/(mmol·h) (R^2 = 0.95) after a cutoff filter was applied to remove the UV

DOI: 10.1021/acs.est.7b00654
Environ. Sci. Technol. 2017, 51, 6877−6886

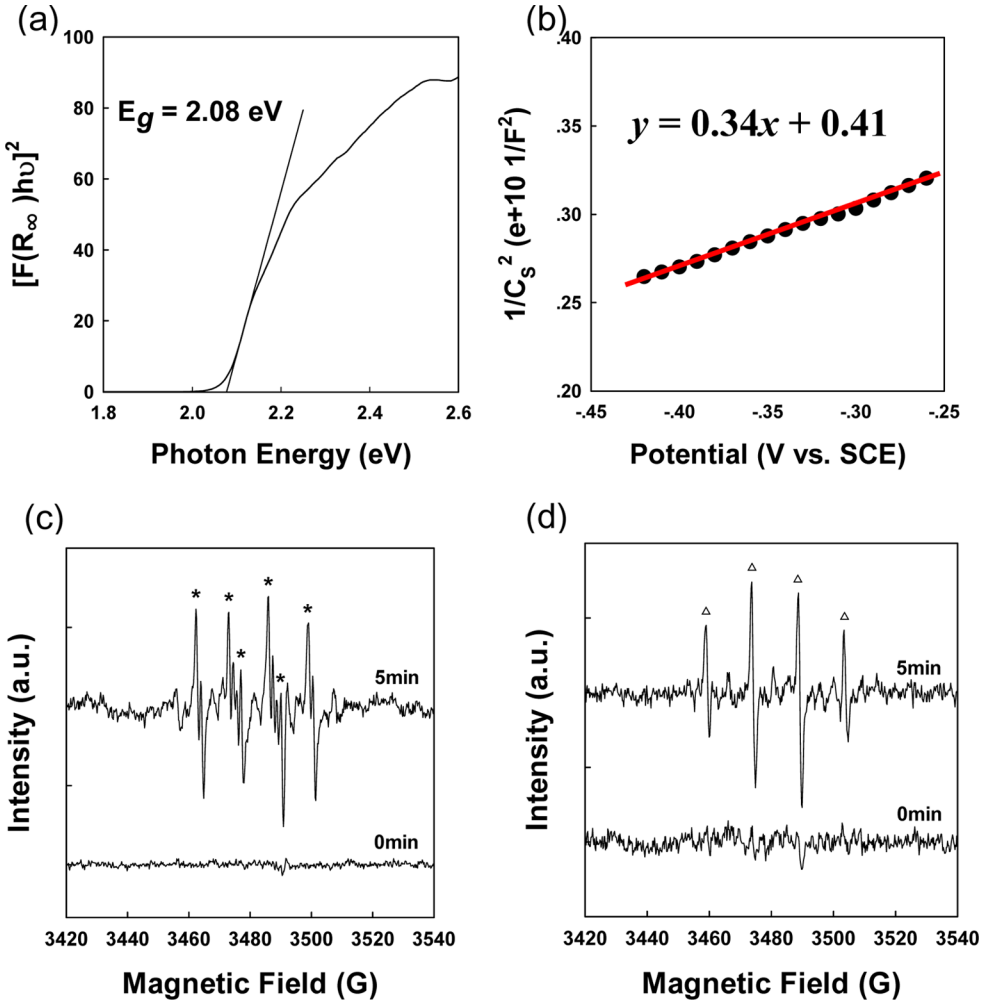

Figure 4. (a) Kubelka–Munk function, $(F(R_\infty)h\upsilon)^2$, as a function of photon energy. (b) Mott–Schottky plot of the commercial cadmium sulfoselenide pigment. (c) ESR spectra recorded under simulated sunlight irradiation with 10 mg/L commercial cadmium sulfoselenide pigment and 100 mM spin trap DMPO in 80% DMSO, indicating the generation of superoxide ($O_2^{\bullet-}$). (d) ESR spectra recorded during simulated sunlight irradiation with 10 mg/L commercial cadmium sulfoselenide pigment and 100 mM spin trap DMPO in water, indicating the generation of hydroxyl radicals (•OH).

component of the simulated sunlight (Figure 1a). This indicates that the photodissolution can be induced by visible light in the solar spectrum which comprises the majority of the photon flux in solar irradiation.[39]

During irradiation, the color of the cadmium sulfoselenide pigment suspension changed from red to transparent, supporting the fast photodissolution of the pigment (Figure 1b). The ζ-potential of the pigment particles was stable at −26.15 ± 1.24 mV (Figure S4). TEM and SEM micrographs of pigment particles suggest that particle size was significantly decreased owing to the photodissolution process (Figure 2a–d). On the basis of the size distribution diagrams (Figure 2e,f), the number-average size of the pigment particles sharply decreased from 186.1 ± 95.8 nm to 19.7 ± 8.7 nm after 7-h irradiation. The size distribution also became narrower (i.e., less heterogeneous) after irradiation. The majority of the 7-h-irradiated pigment particles had sizes within the range of 10–20 nm.

The release of sulfur and selenium species and their mass balance were examined during the photodissolution of commercial cadmium sulfoselenide pigment (Figure 3). The solution concentration of SO_4^{2-} increased with decreasing sulfur remaining in the pigment (Figure 3a). No SO_3^{2-} or S was detected using ion chromatography and HPLC, respectively. The mass balance of sulfur species was 81.8% at 24 h. Similar analysis was applied to selenium species (Figure 3b). Both SeO_3^{2-} and SeO_4^{2-} were detected as reaction products, with SeO_4^{2-} being the major product and SeO_3^{2-} being the intermediate product. The mass balance of selenium species was 83.1% at 24 h.

Mechanisms of the Photodissolution of Commercial Cadmium Sulfoselenide Pigments. To better understand the photochemistry of commercial cadmium sulfoselenide pigment in the solar spectrum, its band gap energy (E_g) was determined by DRS (Figure 4a). The commercial pigment showed strong light absorbance up to ∼600 nm. Its DRS spectrum was transformed to the Kubelka–Munk function, $(F(R_\infty)h\upsilon)^2$, versus the photon energy plot as shown in Figure 4a.[40,41]

$$F(R_\infty) = (1 - R)^2/(2R) \quad (1)$$

in which, R is the reflectance, h is Planck's constant, and υ is the light frequency. The E_g was determined to be 2.08 eV by extrapolating the steepest slope to the x axis (Figure 4b).[41] This

DOI: 10.1021/acs.est.7b00654
Environ. Sci. Technol. 2017, 51, 6877–6886

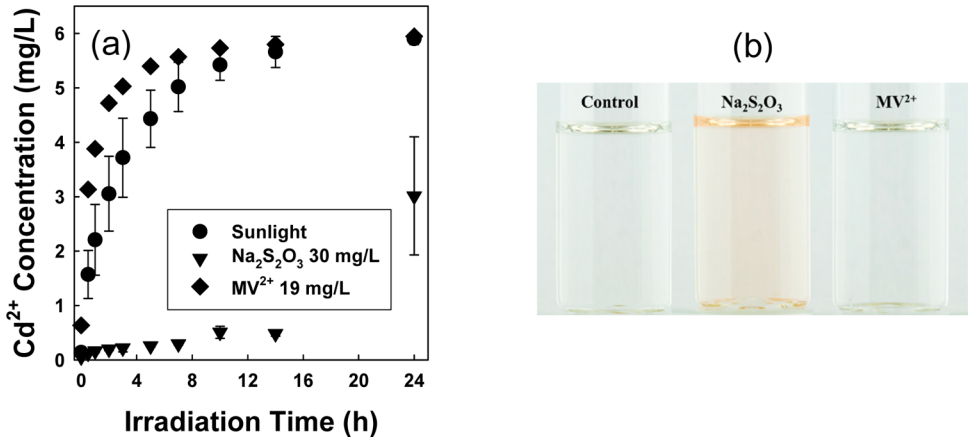

Figure 5. (a) Cadmium release kinetics of 10 mg/L commercial cadmium sulfoselenide pigment in 1 mM NaCl solution at initial pH of 6.86 ± 0.43 in the presence of 30 mg/L $Na_2S_2O_3$ or 19 mg/L methyl viologen (MV^{2+}) under simulated sunlight (202 mW/cm^2). Error bars represent ± one standard deviation from the average of triplicate tests. (b) Photos of 10 mg/L commercial cadmium sulfoselenide pigment in 1 mM NaCl solution in the presence of 30 mg/L $Na_2S_2O_3$ or 19 mg/L MV^{2+} after 24 h simulated sunlight irradiation.

value is generally consistent with the typical range of the E_g of cadmium sulfoselenide nanocrystals.[9] Thus, commercial cadmium sulfoselenide pigment used in this study can be activated by irradiation wavelength <596 nm (i.e., 2.08 eV), which covers the major part of the solar spectrum. This agrees well with the fact that the photodissolution kinetics was still fast after filtering the UV light in the simulated sunlight (Figure 1a).

The flat-band potential of the pigment was determined using the Mott−Schottky method (Figure 4b). The slope of the linear regression is positive, indicating that the cadmium sulfoselenide pigment is an n-type semiconductor, for which the flat-band potential is close to the conduction band potential.[42] The conduction band potential of the cadmium pigment used in this study is −0.97 V vs NHE (i.e., −1.21 V vs SCE) at pH 5.5 as determined by the linear extrapolation method. The position of conduction band edge is a function of the solution pH, ~0.059 V/pH.[43] Thus, the conduction band potential is estimated to be −1.06 V at pH 7.0. The valence band is calculated to be 1.02 V based on the conduction band potential and E_g. When excited by incident photons with energy higher than the band gap energy, cadmium sulfoselenide pigment generates electron−hole pairs which migrate to the surface of particles (eq 2).

$$CdS_xSe_{1-x} \xrightarrow{(\lambda<596\ nm)} e^- + h^+ \quad (2)$$

$$e^- + O_2 \rightarrow O_2^{\bullet-} \quad (3)$$

$$2O_2^{\bullet-} + 2H^+ \rightarrow H_2O_2 + O_2 \quad (4)$$

$$H_2O_2 + e^- \rightarrow \bullet OH + OH^- \quad (5)$$

$$H_2O_2 + O_2^{\bullet-} \rightarrow \bullet OH + OH^- + O_2 \quad (6)$$

$$H_2O_2 \xrightarrow{h\upsilon} 2\bullet OH \quad (7)$$

Colloidal semiconductors usually contain a large number of surface defect sites, which can trap charge carriers upon excitation.[44] Some of these charge carriers will react with surrounding molecules to form phototransients. The conduction band potential of the pigment is more negative than the redox potential of O_2/ $O_2^{\bullet-}$ (−0.28 V vs NHE), thus the photogenerated electrons can transfer to O_2 and form $O_2^{\bullet-}$. We carried out ESR experiments under simulated sunlight irradiation using DMPO as a spin trap to detect these phototransients. In the presence of 10 mg/L pigment and 80% DMSO as the •OH quencher, a characteristic fingerprint of the DMPO•OO(H) adduct (a_N = 12.7 G, a_H = 10.3 G) was observed, indicating the generation of $O_2^{\bullet-}$ (Figure 4c).[45] Control test suggested that there was no ESR peaks in the same sample without simulated sunlight irradiation. Thus, the electrons generated by the pigment can combine with oxygen molecules to yield $O_2^{\bullet-}$ (eq 3). The production of $O_2^{\bullet-}$ was also examined by molecular probe, XTT, which can readily react with $O_2^{\bullet-}$, producing XTT formazan.[31] The formation of XTT formazan in the pigment suspension was a function of irradiation time (Figure S5a). It is worth noting that the XTT assay might not be specific to $O_2^{\bullet-}$ in some cases under UV irradiation.[46] Nevertheless, the generation of XTT formazan was almost completely inhibited in the presence of superoxide dismutase (Figure S5b), confirming the generation of $O_2^{\bullet-}$.[46]

In 10 mg/L pigment water suspension, we observed an ESR pattern consisting of a 1:2:2:1 quartet with a_N = a_H = 14.9 G under simulated sunlight, which is the hallmark for the DMPO•OH adduct (Figure 4d), indicating the generation of •OH.[45] By using molecular probe, *p*CBA, the generation of •OH was confirmed in the illuminated pigment suspension (Figure S5c).[32,33] The valence band potential of the pigment (+1.02 V vs NHE) is lower than the redox potential of •OH/ H_2O (+2.27 V vs NHE) and •OH/OH^- (+1.99 V vs NHE). Thus, the generation of •OH was not caused by the reactions between holes and H_2O or surface-bound OH^-. H_2O_2 was detected in the irradiated pigment suspension as shown in Figure S5d, which was the product of the disproportionation of $O_2^{\bullet-}$ (eq 4). Therefore, the detected •OH was most likely formed through the H_2O_2 reduction pathway (eq 5-6).[47]

The valence band edge (+1.02 V vs NHE) is higher than the standard potential for anodic dissolution of cadmium chalcogenide, around +0.32 V vs NHE,[48] leading to the corrosion of pigment surface sites by photogenerated holes.[15,19,49,50] To test this hypothesis, we added electron/ hole scavengers into the reaction system. The photodissolution of the pigment was completely inhibited initially by the addition of 30 mg/L $Na_2S_2O_3$, a hole scavenger,[51] highlighting the predominant role of photogenerated holes (Figure 5). The release of Cd^{2+} was observed after 7-h irradiation likely due to the consumption of $Na_2S_2O_3$. However, the photodissolution of

DOI: 10.1021/acs.est.7b00654
Environ. Sci. Technol. 2017, 51, 6877−6886

Cd^{2+} was enhanced in the presence of an electron scavenger, MV^{2+} (Figure 5).[15] The MV^{2+} quickly reacted with photogenerated electrons, decreasing the recombination of photogenerated electron−hole pairs and consequently leaving more holes involved in the reactions with pigment lattices.[15,22] On the basis of the evidence presented above as well as earlier reports on the photocorrosion of CdS and CdSe nanocrystals, we proposed a mechanism for the sunlight-induced dissolution of commercial cadmium sulfoselenide pigments:

$$CdS_xSe_{1-x} + 4h^+ + O_2 + 2H_2O \xrightarrow{(\lambda<596\ nm)} Cd^{2+} + xSO_4^{2-} + 4H^+ + (1-x)SeO_4^{2-} \quad (8)$$

Impact of Water Chemistry on the Photodissolution Kinetics of Commercial Cadmium Sulfoselenide Pigments. To better discern the environmentally relevant release process, the impact of solution chemistry including pH, phosphate, carbonate, and tannic acid on the photodissolution kinetics was further examined. The photodissolution process was highly pH-dependent (Figure 6a). There was no significant change of the photodissolution rate in acidic conditions as the initial pH increased from 4.92 ± 0.03 to 6.95 ± 0.02. However, photodissolution drastically decreased as the initial pH increased from 6.95 ± 0.02 to 10.06 ± 0.02. This could be attributed to the reduced valence band edge of the pigment, which decreases from +1.02 V (NHE) to +0.84 V (NHE) as pH increases from 7 to 10. Nevertheless, the photogenerated holes are still able to oxidize the cadmium pigment at pH 10 since the standard potential for anodic dissolution of cadmium chalcogenide is around +0.32 V vs NHE.[43,48] Another potential offsetting mechanism is the formation of $Cd(OH)_2$ precipitates (K_{sp}, $Cd(OH)_2$ = 7.2 × 10^{-15})[52] or sorption of OH^- on the particle surfaces under alkaline conditions.[50] These processes effectively blocked the surface sites suitable for trapping holes, leading to higher recombination of excitons and consequently less reaction with surface trapped holes.[22] Consistently, the XPS measurements suggest the atomic ratio of oxygen in hydroxide to cadmium on the pigment surface increased from 34.2% to 55.0% after 1 h irradiation at pH 10 (Figure S6). For experiments done at initial pH of 10.06 ± 0.02, the photodissolution process was slow during the initial 2 h, and then drastically increased afterward. This is because the overall reaction releases protons (eq 8) and lowers the pH of the system, facilitating the photodissolution process. The final pH of the samples with initial pH of 10.06 ± 0.02 was 6.81 ± 0.09, consistent with this argument.

Naturally occurring anions including phosphate and carbonate significantly affected the photodissolution process. The release of Cd^{2+} from cadmium sulfoselenide pigment during simulated sunlight irradiation was inhibited in the presence of 10 mg/L phosphate or carbonate species (Figure 6b). The inhibitory effect of phosphate and carbonate was exacerbated as their concentration was further increased to 200 mg/L. The inhibition mechanism is the formation of photostable cadmium salts, which are highly insoluble in water (K_{sp}, $Cd_3(PO_4)_2$ = 2.5 × 10^{-33}, and K_{sp}, $CdCO_3$ = 5.7 × 10^{-13}).[53,54] Meanwhile, the anions in these cadmium salts, PO_4^{3-} and CO_3^{2-}, cannot be oxidized by photogenerated holes. As a result, these insoluble and photostable cadmium salts can passivate the pigment surface, inhibiting the oxidation of cadmium sulfoselenide and the consequent release of Cd^{2+}.

The presence of 20 mg/L tannic acid, a surrogate for dissolved organic matter (DOM),[55] inhibited the photodissolution of cadmium sulfoselenide pigment. The inhibitory effect can be attributed to two mechanisms. Tannic acid molecules can absorb light, exerting a screening effect. This decreases the amount of photons received by pigment particles and consequently hinders the photodissolution process. Furthermore, tannic acid is a plant polyphenol with antioxidant properties.[56] It can scavenge photogenerated holes, mitigating oxidation of the pigment.[57] However, photoactive DOM can

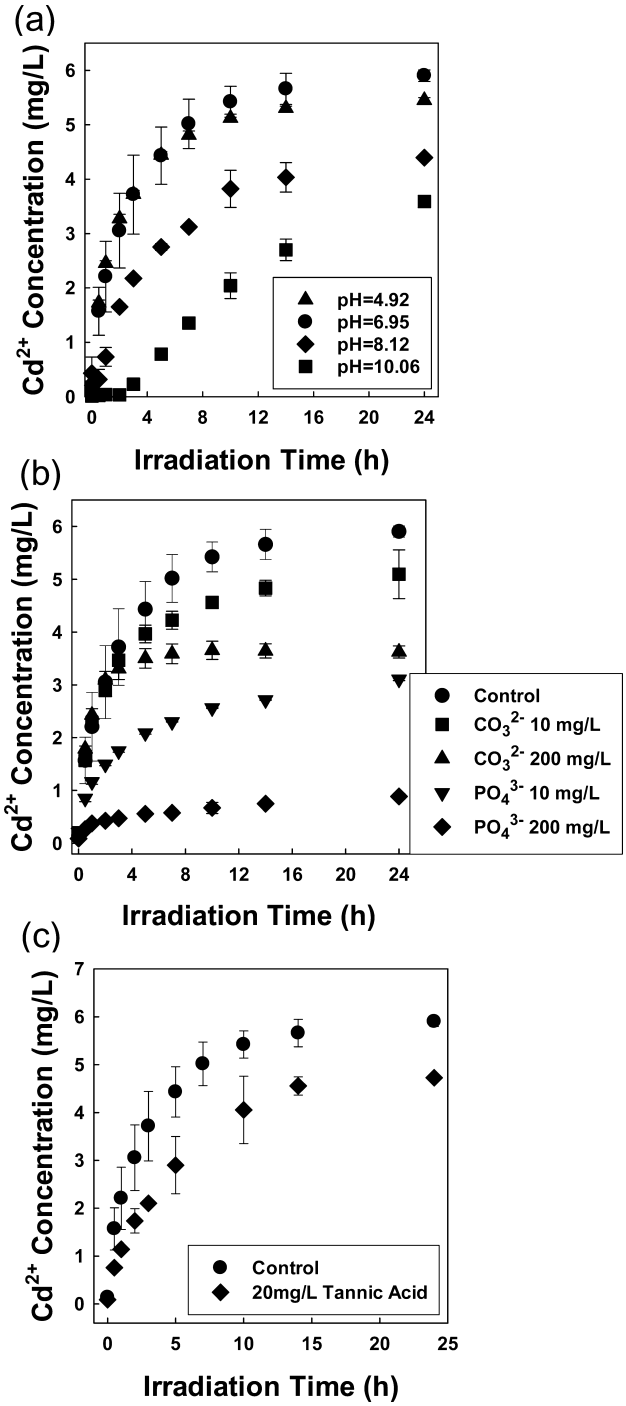

Figure 6. Dissolution kinetics of 10 mg/L commercial cadmium sulfoselenide pigment in 1 mM NaCl solution under simulated sunlight irradiation (a) at various initial pH, (b) in the presence of PO_4^{3-} or CO_3^{2-} species at initial pH of 6.90 ± 0.30, and (c) in the presence of tannic acid at initial pH of 6.51 ± 0.10. Error bars represent ± one standard deviation from the average of triplicate tests.

DOI: 10.1021/acs.est.7b00654
Environ. Sci. Technol. 2017, 51, 6877−6886

produce phototransients such as singlet oxygen, hydrogen peroxide, hydroxyl radical, and superoxide,[58] which could enhance the oxidative dissolution of pigment particles. The overall effect of photoactive DOM will depend on the interplay of its screening, hole scavenging, and photoactivity.

Photodissolution of Commercial Cadmium Sulfoselenide Pigment in a Natural Setting. In order to gain further insight into the natural photodissolution process of commercial cadmium sulfoselenide pigment, we carried out a solar irradiation experiment with a river water sample on the campus of Nanjing University from 11 a.m. to 3 p.m. on 11/04/2016. The solar irradiance was in the range of 35.8 to 56.1 mW/cm^2 (Figure S7). The natural river water had pH of 7.70 ± 0.20 and total organic carbon of 3.99 ± 0.32 mg/L. The concentrations of phosphate and carbonate ions in the river water were 0.65 ± 0.04 mg/L and 271.87 ± 9.34 mg/L, respectively. Fast release kinetics of Cd^{2+} was observed in this river water sample under natural solar irradiation, with 38.6 ± 0.1% of the cadmium in the pigment being released within 4 h (Figure S8). Thus, we provide unequivocal evidence of fast and significant cadmium release from commercial cadmium sulfoselenide pigments under natural conditions.

Environmental Implications. The commercial cadmium sulfoselenide pigment is photoactive under solar irradiation and is susceptible to photodissolution, which is the key environmental process controlling its release of Cd^{2+}. The release can be mitigated by an increase in pH and the presence of anions that can form insoluble and photostable salts with Cd^{2+}. Once released into aquatic systems, commercial cadmium pigment will undergo significant photodissolution within short period of time. The majority part of it will not persist in the particulate form in natural settings, but will convert to highly toxic and bioavailable Cd^{2+}. Thus, current risk assessments and regulations of cadmium pigments and other semiconductor pigments with hazardous metals need to consider their photochemistry. Our ongoing field investigation and a previous study[59] show extensive use and potential discharge of cadmium pigments in several Chinese cities with a booming ceramic industry. We postulate that photodissolution is one of the environmental processes that lead to the significant accumulation of cadmium in soils at several sites in these cities. Furthermore, sunlight exposure of materials containing cadmium pigments could lead to potential environmental risks and health concerns. Little is known about the extent to which the matrix such as polymers and ceramics can inhibit the photodissolution of cadmium pigments and the subsequent release of metals. Future research is needed to quantify the photoinduced release of toxic Cd^{2+} from colored products containing cadmium pigments.

■ ASSOCIATED CONTENT

Supporting Information

The Supporting Information is available free of charge on the ACS Publications website at DOI: 10.1021/acs.est.7b00654.

The experimental setup for irradiation experiments, the spectrum of the Xeon lamp used in this study and solar irradiation, the photodissolution kinetics of commercial cadmium sulfoselenide pigments from different vendors, the ζ-potential of the commercial cadmium sulfoselenide pigment as a function of irradiation time, the detection of $O_2^{\bullet-}$, •OH, and H_2O_2 using probe molecules, the XPS spectrum of the O 1s peak of the pigment at different conditions, the variation of solar light power density during the natural light exposure, the dissolution kinetics of commercial cadmium sulfoselenide pigment in natural river water sample under solar irradiation, the cadmium release kinetics of the pigment under dark condition at initial pH of 4.92, and the determination of pseudo-second-order reaction rate constant (PDF)

■ AUTHOR INFORMATION

Corresponding Author

*Phone: +86-025-8968-0256; e-mail: xiaoleiqu@nju.edu.cn (X.Q.).

ORCID

Mingce Long: 0000-0002-5168-8330
Pedro J. J. Alvarez: 0000-0002-6725-7199
Shourong Zheng: 0000-0001-8660-4910
Xiaolei Qu: 0000-0002-9157-4274
Dongqiang Zhu: 0000-0001-6190-5522

Notes

The authors declare no competing financial interest.

■ ACKNOWLEDGMENTS

This work was supported by the National Key Basic Research Program of China (Grant 2014CB441103), the National Natural Science Foundation of China (Grant 21622703, 21407073, 21225729, 21237002, and 21507056), the Department of Science and Technology of Jiangsu Province (BE2015708), and the NSF ERC on Nanotechnology-Enabled Water Treatment (EEC-1449500). We thank the State Key Laboratory of Environmental Chemistry and Ecotoxicology, Research Center for Eco-Environmental Sciences, Chinese Academy of Sciences for partial funding (KF2014-11).

■ REFERENCES

(1) Jansen, M.; Letschert, H. P. Inorganic yellow-red pigments without toxic metals. *Nature* **2000**, *404*, 980−982.

(2) Faulkner, E. B.; Schwartz, R. J. *High Performance Pigments*; John Wiley & Sons: New York, 2009.

(3) EPA, Cadmium iris summary. *CASRN 7440-43-9* 1987.

(4) Lu, Z. Z.; Xu, J.; Xie, X.; Wang, H. K.; Wang, C. D.; Kwok, S. Y.; Wong, T.; Kwong, H. L.; Bello, I.; Lee, C. S.; Lee, S. T.; Zhang, W. J. CdS/CdSe double-sensitized ZnO nanocable arrays synthesized by chemical solution method and their photovoltaic applications. *J. Phys. Chem. C* **2012**, *116*, 2656−2661.

(5) WAI, Ltd. *Assessment of the risks to health and to the environment of cadmium contained in certain products and of the effects of further restrictions on their marketing and use*, 1998.

(6) Wilson, D. C.; Young, P. J.; Hudson, B. C.; Baldwin, G. Leaching of cadmium from pigmented plastics in a landfill site. *Environ. Sci. Technol.* **1982**, *16*, 560−566.

(7) Fleig, I.; Rieth, H.; Stocker, W. G.; Thiess, A. M. Chromosome investigations of workers exposed to cadmium in the manufacturing of cadmium stabilizers and pigments. *Ecotoxicol. Environ. Saf.* **1983**, *7*, 106−110.

(8) Kawasaki, T.; Kono, K.; Dote, T.; Usuda, K.; Shimizu, H.; Dote, E. Markers of cadmium exposure in workers in a cadmium pigment factory after changes in the exposure conditions. *Toxicol. Ind. Health* **2004**, *20*, 51−56.

(9) Swafford, L. A.; Weigand, L. A.; Bowers, M. J.; McBride, J. R.; Rapaport, J. L.; Watt, T. L.; Dixit, S. K.; Feldman, L. C.; Rosenthal, S. J. Homogeneously alloyed CdS_xSe_{1-x} nanocrystals: Synthesis, characterization, and composition/size-dependent band gap. *J. Am. Chem. Soc.* **2006**, *128*, 12299−12306.

DOI: 10.1021/acs.est.7b00654
Environ. Sci. Technol. 2017, 51, 6877−6886

(10) Eastaugh, N.; Walsh, V.; Chaplin, T.; Siddall, R. *Pigment Compendium: A Dictionary of Historical Pigments*; Routledge: London, 2007.
(11) Mane, R. S.; Lokhande, C. D. Studies on chemically deposited cadmium sulphoselenide (CdSSe) films. *Thin Solid Films* **1997**, *304*, 56−60.
(12) Khot, K. V.; Mali, S. S.; Pawar, N. B.; Kharade, R. R.; Mane, R. M.; Patil, P. B.; Patil, P. S.; Hong, C. K.; Kim, J. H.; Heo, J.; Bhosale, P. N. Simplistic construction of cadmium sulfoselenide thin films via a hybrid chemical process for enhanced photoelectrochemical performance. *RSC Adv.* **2015**, *5*, 40283−40296.
(13) Hossain, M. A.; Jennings, J. R.; Mathews, N.; Wang, Q. Band engineered ternary solid solution CdS_xSe_{1-x}-sensitized mesoscopic TiO_2 solar cells. *Phys. Chem. Chem. Phys.* **2012**, *14*, 7154−7161.
(14) Li, Y.; Zhang, W.; Li, K.; Yao, Y.; Niu, J.; Chen, Y. Oxidative dissolution of polymer-coated CdSe/ZnS quantum dots under uv irradiation: Mechanisms and kinetics. *Environ. Pollut.* **2012**, *164*, 259−266.
(15) Matsumoto, H.; Sakata, T.; Mori, H.; Yoneyama, H. Preparation of monodisperse CdS nanocrystals by size selective photocorrosion. *J. Phys. Chem.* **1996**, *100*, 13781−13785.
(16) Spathis, P.; Poulios, I. The corrosion and photocorrosion of zinc and zinc oxide coatings. *Corros. Sci.* **1995**, *37*, 673−680.
(17) Peng, X.; Schlamp, M. C.; Kadavanich, A. V.; Alivisatos, A. P. Epitaxial growth of highly luminescent CdSe/CdS core/shell nanocrystals with photostability and electronic accessibility. *J. Am. Chem. Soc.* **1997**, *119*, 7019−7029.
(18) Xu, L.; Chen, K.; El-Khair, H. M.; Li, M.; Huang, X. Enhancement of band-edge luminescence and photo-stability in colloidal CdSe quantum dots by various surface passivation technologies. *Appl. Surf. Sci.* **2001**, *172*, 84−88.
(19) Toma, F. M.; Cooper, J. K.; Kunzelmann, V.; McDowell, M. T.; Yu, J.; Larson, D. M.; Borys, N. J.; Abelyan, C.; Beeman, J. W.; Yu, K. M.; Yang, J.; Chen, L.; Shaner, M. R.; Spurgeon, J.; Houle, F. A.; Persson, K. A.; Sharp, I. D. Mechanistic insights into chemical and photochemical transformations of bismuth vanadate photoanodes. *Nat. Commun.* **2016**, *7*, 12012.
(20) Fermín, D. J.; Ponomarev, E. A.; Peter, L. M. A kinetic study of CdS photocorrosion by intensity modulated photocurrent and photoelectrochemical impedance spectroscopy. *J. Electroanal. Chem.* **1999**, *473*, 192−203.
(21) Meissner, D.; Memming, R.; Kastening, B. Photoelectrochemistry of cadmium sulfide. 1. Reanalysis of photocorrosion and flat-band potential. *J. Phys. Chem.* **1988**, *92*, 3476−3483.
(22) Spanhel, L.; Haase, M.; Weller, H.; Henglein, A. Photochemistry of colloidal semiconductors 0.20. Surface modification and stability of strong luminescing CdS particles. *J. Am. Chem. Soc.* **1987**, *109*, 5649−5655.
(23) Manner, V. W.; Koposov, A. Y.; Szymanski, P.; Klimov, V. I.; Sykora, M. Role of solvent−oxygen ion pairs in photooxidation of CdSe nanocrystal quantum dots. *ACS Nano* **2012**, *6*, 2371−2377.
(24) Xi, L. F.; Lek, J. Y.; Liang, Y. N.; Boothroyd, C.; Zhou, W. W.; Yan, Q. Y.; Hu, X.; Chiang, F. B. Y.; Lam, Y. M. Stability studies of CdSe nanocrystals in an aqueous environment. *Nanotechnology* **2011**, *22*, 275706.
(25) Derfus, A. M.; Chan, W. C. W.; Bhatia, S. N. Probing the cytotoxicity of semiconductor quantum dots. *Nano Lett.* **2004**, *4*, 11−18.
(26) Shang, E.; Niu, J.; Li, Y.; Zhou, Y.; Crittenden, J. C. Comparative toxicity of Cd, Mo, and W sulphide nanomaterials toward *E. coli* under UV irradiation. *Environ. Pollut.* **2017**, *224*, 606−614.
(27) Meissner, D.; Memming, R.; Shuben, L.; Yesodharan, S.; Grätzel, M. Photocorrosion by oxygen uptake in aqueous cadmium sulphide suspensions. *Berichte der Bunsengesellschaft für physikalische Chemie* **1985**, *89*, 121−124.
(28) Anaf, W.; Trashin, S.; Schalm, O.; van Dorp, D.; Janssens, K.; De Wael, K. Electrochemical photodegradation study of semiconductor pigments: Influence of environmental parameters. *Anal. Chem.* **2014**, *86*, 9742−9748.
(29) Van der Snickt, G.; Dik, J.; Cotte, M.; Janssens, K.; Jaroszewicz, J.; De Nolf, W.; Groenewegen, J.; Van der Loeff, L. Characterization of a degraded cadmium yellow (CdS) pigment in an oil painting by means of synchrotron radiation based X-ray techniques. *Anal. Chem.* **2009**, *81*, 2600−2610.
(30) Van der Snickt, G.; Janssens, K.; Dik, J.; De Nolf, W.; Vanmeert, F.; Jaroszewicz, J.; Cotte, M.; Falkenberg, G.; Van der Loeff, L. Combined use of synchrotron radiation based micro-X-ray fluorescence, micro-X-ray diffraction, micro-X-ray absorption near-edge, and micro-fourier transform infrared spectroscopies for revealing an alternative degradation pathway of the pigment cadmium yellow in a painting by Van Gogh. *Anal. Chem.* **2012**, *84*, 10221−10228.
(31) Sutherland, M. W.; Learmonth, B. A. The tetrazolium dyes MTS and XTT provide new quantitative assays for superoxide and superoxide dismutase. *Free Radical Res.* **1997**, *27*, 283−289.
(32) Haag, W. R.; Hoigné, J. Photo-sensitized oxidation in natural water via •OH radicals. *Chemosphere* **1985**, *14*, 1659−1671.
(33) Zepp, R. G.; Schlotzhauer, P. F.; Sink, R. M. Photosensitized transformations involving electronic-energy transfer in natural-waters - role of humic substances. *Environ. Sci. Technol.* **1985**, *19*, 74−81.
(34) Chen, C.-Y.; Jafvert, C. T. Photoreactivity of carboxylated single-walled carbon nanotubes in sunlight: Reactive oxygen species production in water. *Environ. Sci. Technol.* **2010**, *44*, 6674−6679.
(35) Hsieh, H. S.; Wu, R. R.; Jafvert, C. T. Light-independent reactive oxygen species (ROS) formation through electron transfer from carboxylated single-walled carbon nanotubes in water. *Environ. Sci. Technol.* **2014**, *48*, 11330−11336.
(36) Derjaguin, B.; Landau, L. Theory of stability of highly charged liophobic sols and adhesion of highly charged particles in solutions of electrolytes. *Zh. Eksp. Teor. Fiz.* **1945**, *15*, 663−682.
(37) Verwey, E. J. W. Theory of the stability of lyophobic colloids. *J. Phys. Colloid Chem.* **1947**, *51*, 631−636.
(38) Kevin, P.; Alghamdi, Y. G.; Lewis, D. J.; Azad Malik, M. Morphology and band gap controlled AACVD of CdSe and CdS_xSe_{1-x} thin films using novel single source precursors: Bis(diethyldithio/diselenocarbamato)cadmium(II). *Mater. Sci. Semicond. Process.* **2015**, *40*, 848−854.
(39) Zou, Z.; Ye, J.; Sayama, K.; Arakawa, H. Direct splitting of water under visible light irradiation with an oxide semiconductor photocatalyst. *Nature* **2001**, *414*, 625−627.
(40) Kubelka, P. New contributions to the optics of intensely light-scattering materials. Part I. *J. Opt. Soc. Am.* **1948**, *38*, 448−457.
(41) López, R.; Gómez, R. Band-gap energy estimation from diffuse reflectance measurements on sol−gel and commercial TiO_2: A comparative study. *J. Sol-Gel Sci. Technol.* **2012**, *61*, 1−7.
(42) Bott, A. W. Electrochemistry of semiconductors. *Curr. Sep.* **1998**, *17*, 87−92.
(43) Xu, Y.; Schoonen, M. A. A. The absolute energy positions of conduction and valence bands of selected semiconducting minerals. *Am. Mineral.* **2000**, *85*, 543−556.
(44) Kamat, P. V. Photochemistry on nonreactive and reactive (semiconductor) surfaces. *Chem. Rev.* **1993**, *93*, 267−300.
(45) Makino, K.; Hagiwara, T.; Murakami, A. A mini review: Fundamental aspects of spin trapping with dmpo. *International Journal of Radiation Applications and Instrumentation. Part C. Radiation Physics and Chemistry* **1991**, *37*, 657−665.
(46) Zhao, J. F.; Zhang, B. W.; Li, J. Y.; Liu, Y. C.; Wang, W. F. Photo-enhanced oxidizability of tetrazolium salts and its impact on superoxide assaying. *Chem. Commun.* **2016**, *52*, 11595−11598.
(47) Kim, J.; Lee, C. W.; Choi, W. Platinized WO_3 as an environmental photocatalyst that generates OH radicals under visible light. *Environ. Sci. Technol.* **2010**, *44*, 6849−6854.
(48) Bard, A. J.; Wrighton, M. S. Thermodynamic potential for the anodic dissolution of n-type semiconductors. *J. Electrochem. Soc.* **1977**, *124*, 1706−1710.

DOI: 10.1021/acs.est.7b00654
Environ. Sci. Technol. 2017, 51, 6877−6886

(49) Tan, Y.; Jin, S.; Hamers, R. J. Influence of hole-sequestering ligands on the photostability of CdSe quantum dots. *J. Phys. Chem. C* **2013**, *117*, 313−320.
(50) Torimoto, T.; Nishiyama, H.; Sakata, T.; Mori, H.; Yoneyama, H. Characteristic features of size-selective photoetching of CdS nanoparticles as a means of preparation of monodisperse particles. *J. Electrochem. Soc.* **1998**, *145*, 1964−1968.
(51) Belabed, C.; Rekhila, G.; Doulache, M.; Zitouni, B.; Trari, M. Photo-electrochemical characterization of polypyrrol: Application to visible light induced hydrogen production. *Sol. Energy Mater. Sol. Cells* **2013**, *114*, 199−204.
(52) Lide, D. R. *CRC Handbook of Chemistry and Physics*; CRC Press: Boca Raton, FL, 2004; Vol. *85*.
(53) Eighmy, T. T.; Eusden, J. D.; Krzanowski, J. E.; Domingo, D. S.; Staempfli, D.; Martin, J. R.; Erickson, P. M. Comprehensive approach toward understanding element speciation and leaching behavior in municipal solid waste incineration electrostatic precipitator ash. *Environ. Sci. Technol.* **1995**, *29*, 629−646.
(54) Street, J. J.; Lindsay, W. L.; Sabey, B. R. Solubility and plant uptake of cadmium in soils amended with cadmium and sewage sludge. *J. Environ. Qual.* **1977**, *6*, 72−77.
(55) Yamamoto, H.; Liljestrand, H. M.; Shimizu, Y.; Morita, M. Effects of physical−chemical characteristics on the sorption of selected endocrine disruptors by dissolved organic matter surrogates. *Environ. Sci. Technol.* **2003**, *37*, 2646−2657.
(56) Hagerman, A. E.; Riedl, K. M.; Jones, G. A.; Sovik, K. N.; Ritchard, N. T.; Hartzfeld, P. W.; Riechel, T. L. High molecular weight plant polyphenolics (tannins) as biological antioxidants. *J. Agric. Food Chem.* **1998**, *46*, 1887−1892.
(57) Long, M.; Brame, J.; Qin, F.; Bao, J.; Li, Q.; Alvarez, P. J. J. Phosphate changes effect of humic acids on TiO_2 photocatalysis: From inhibition to mitigation of electron−hole recombination. *Environ. Sci. Technol.* **2017**, *51*, 514−521.
(58) Zhou, H.; Lian, L.; Yan, S.; Song, W. Insights into the photo-induced formation of reactive intermediates from effluent organic matter: The role of chemical constituents. *Water Res.* **2017**, *112*, 120−128.
(59) Liao, Q. L.; Liu, C.; Wu, H. Y.; Jin, Y.; Hua, M.; Zhu, B. W.; Chen, K.; Huang, L. Association of soil cadmium contamination with ceramic industry: A case study in a Chinese town. *Sci. Total Environ.* **2015**, *514*, 26−32.

DOI: 10.1021/acs.est.7b00654
Environ. Sci. Technol. 2017, 51, 6877−6886